Improvement of MJO prediction and moistening processes for the DYNAMO period

Takuya KOMORI* and Akihiko SHIMPO

Climate Prediction Division, Japan Meteorological Agency, Tokyo, Japan
Email: komori@met.kishou.go.jp

1. INTRODUCTION

Improvement of Madden-Julian Oscillation (MJO) prediction is crucial for medium- to extended-range predictability in light of the link between operational weather and climate predictions. Whilst every effort has been made to improve the MJO prediction skill of the operational Global Spectral Model (GSM) at the Japan Meteorological Agency (JMA), the results of comparison with special observations conducted during the Dynamics of the Madden-Julian Oscillation (DYNAMO) period over the Indian Ocean suggest a lack of skill in the convectively active phase when dry air intrudes into the eastward propagating MJO. Accordingly, a revision of convection and cloud schemes in the GSM with focus on the moistening processes of the MJO is required.

2. REVISED CONVECTION AND CLOUD SCHEMES

The GSM has the prognostic Arakawa-Schubert (AS) convection scheme with a spectral cloud ensemble and prognostic closure, as well as the large-scale cloud scheme with PDF type based on Smith (1990) with some modifications (JMA 2013). In this study, the following modifications were tested for the schemes:

a) Introduction of new relative-humidity (RH) dependent formulation inspired by Bechtold et al. (2008) for entrainment $\varepsilon(z,t,i)$ in updraft mass flux:

$$\varepsilon(z,t,i) = \varepsilon'(t,i)f\left(\overline{RH}(z)\right)$$
$$f\left(\overline{RH}(z)\right) = (RH_c - 1)\overline{q_s}/\overline{q} + \left(\overline{q_s} - \overline{q}\right)/\overline{q} = \left(RH_c - \overline{RH}(z)\right)/\overline{RH}(z)$$

where the constant parameter $RH_c = 1.1$, and $\varepsilon'(t,i)$ is diagnosed for each convective plume i at every time step t depending on the environmental profile of moist static energy. $\overline{q}$ and $\overline{q_s}$ are the specific humidity and saturation specific humidity in the environment, respectively.

b) Implementation of a resolution-dependent parameter on a convective adjustment time scale:
$$\tau = \alpha\tau_0 \times \exp(\beta \cdot n_T)$$
where n_T is the spectral truncation number of the GSM, and τ_0, α, β are constant parameters.

c) Increased effect of convective momentum transport (CMT) by 20%.

d) Modification of parameters for cloud ice, resulting in less ice falling to the surface.

3. RESULTS

The results of an experiment (TEST) with the revised convection and cloud schemes were compared to those of an experiment (CNTL) based on operational configuration. The low-resolution version of the GSM (TL479L100) was used for both experiments. Figure 1 shows a situation with dry-air intrusion into the middle troposphere during the DYNAMO period at the ARM (atmospheric radiation measurement) Gan Island site. The new RH-dependent formulation for entrainment and the shorter convective adjustment time scale in TEST reproduced the suppressed convection observed when the dry air intruded. The less amount of detrainment from convection in TEST led to a lower RH value in the middle troposphere as also seen in sonde observation, whereas CNTL exhibited persistent errors with a higher RH value in the middle troposphere due to excessive development of deep convection.

During the DYNAMO period, the MJO was initiated over the Indian Ocean and weakened over the Maritime Continent. Hovmöller plots for velocity potential at 200 hPa in one-month prediction for the MJO (Figure 2) demonstrate significantly improved performance in TEST compared with CNTL for the eastward propagation of the divergent flow. The increased effect of CMT in TEST contributed to a deceleration of the eastward propagation of convectively organized cloud clusters. Due to the effect of RH-dependent entrainment, TEST also reproduced the backward-tilt vertical structure of the MJO and resulted in better distribution of specific humidity in the boundary layer (Figure 3). Wavenumber-frequency spectra with an equatorially symmetric component of the OLR simulated over the period from 2001 to 2007 with TL159L100 using SST climatology (Figure 4) revealed an excessive Kelvin wave peak and a significantly weakened signal for the MJO in CNTL. These values were better in TEST, although there is still room for improvement of spectral strength. Overall, the revision of the convection and cloud schemes shows encouraging results with significant improvement of prediction for many aspects of the MJO and related moistening processes. In future work, the characteristics of error growth depending on GSM horizontal resolution will be investigated toward the operational seamless prediction covering from short-range to seasonal time scales.

REFERENCE

Bechtold P., M. Kohler, T. Jung, F. Doblas-Reyes, M. Leutbecher, M. Rodwell, F. Vitart and G. Balsamo, 2008: Advances in simulating atmospheric variability with the ECMWF model: From synoptic to decadal timescales. *Q. J. R. Meteorol. Soc.*, **134**, 1337–1351.

JMA, 2013: Outline of the operational numerical weather prediction at the Japan Meteorological Agency. Appendix to WMO technical progress report on the global data-processing and forecasting system and numerical weather prediction research. 188pp. Available online: http://www.jma.go.jp/jma/jma-eng/jma-center/nwp/outline2013-nwp/index.htm

Smith, R. N. B., 1990: A scheme for predicting layer clouds and their water content in a general circulation model, *Q. J. R. Meteorol. Soc.*, **116**, 435–460.
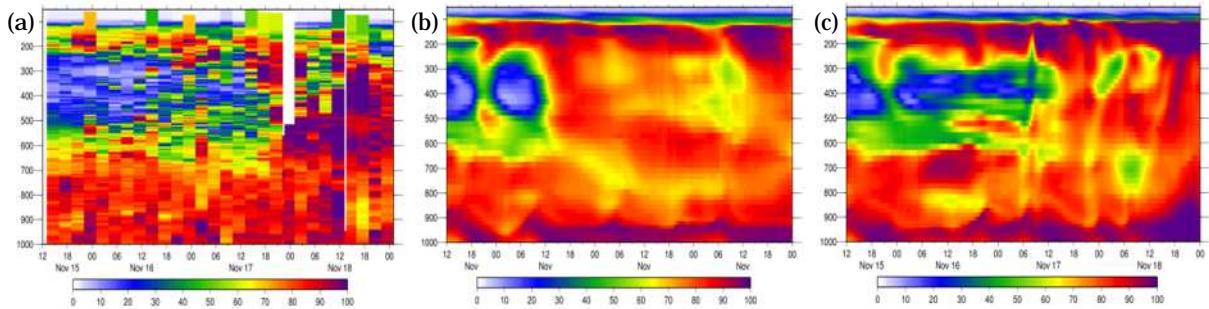
Figure 1. Pressure-time cross section of relative humidity [%] at the ARM Gan Island site for (a) sonde observation and 84-hour simulations of (b) CNTL and (c) TEST with TL479L100 with an initial time of 12 UTC on 15 November 2011
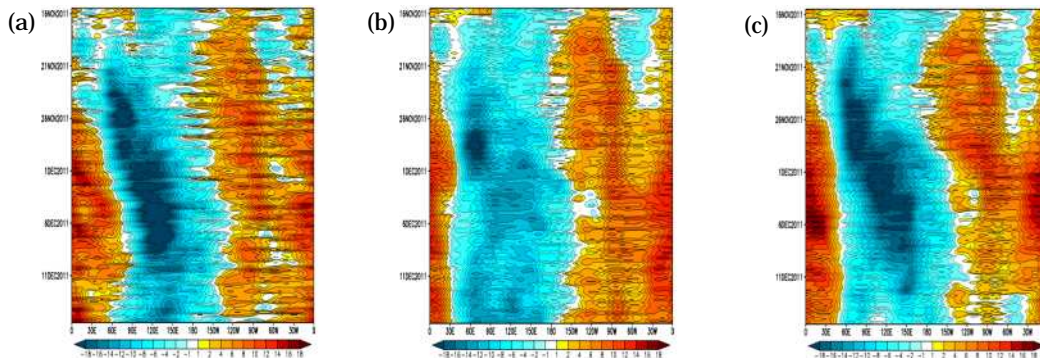
Figure 2. Hovmöller plots of velocity potential at 200 hPa [10^6 m^2 s^{-1}] averaged over 15°S – 15°N: (a) ERA-Interim and one-month simulations of (b) CNTL and (c) TEST with TL479L100 with an initial time of 12 UTC on 15 November 2011
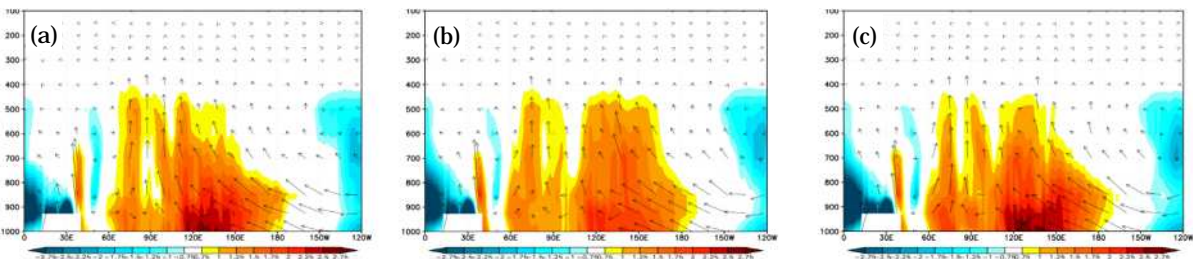
Figure 3. Pressure-longitude cross section of specific humidity [g kg^{-1}] anomaly (shaded) and moisture flux vectors of zonal [m s^{-1} g kg^{-1}] and vertical [Pa s^{-1} g kg^{-1}] components : (a) operational analysis, (b) CNTL and (c) TEST simulations with TL479L100 72-hour forecast with an initial time of 12 UTC on 26 November 2011
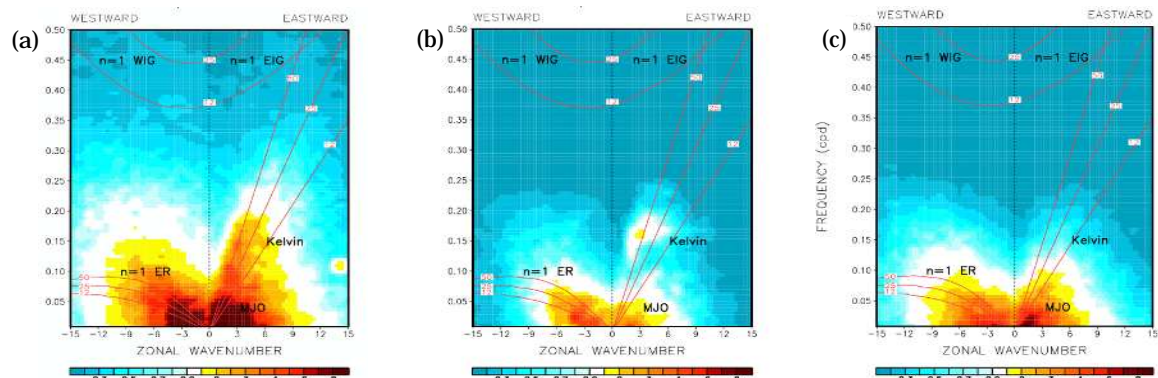
Figure 4. Wavenumber-frequency power spectra with an equatorially symmetric component of the OLR (15°N – 15°S): (a) NOAA AVHRR, (b) CNTL and (c) TEST simulations over the period from 2001 – 2007 with TL159L100 using SST climatology